


Chondral Defects Cause Kissing Lesions in a Porcine Model

CARTILAGE
2021, Vol. 13(Suppl 2) 692S–702S
© The Author(s) 2020
Article reuse guidelines:
sagepub.com/journals-permissions
DOI: 10.1177/1947603520951636
journals.sagepub.com/home/CAR


Wenqiang Yan^{1,*}, Xingquan Xu^{1,*}, Qian Xu¹, Ziyang Sun¹,
Zhongyang Lv¹, Rui Wu¹, Wenjin Yan¹, Qing Jiang^{1,2},
and Dongquan Shi¹ 

Abstract

Objective. To assess the development of kissing lesions 12 months after the generation of full-thickness chondral defects. **Design.** Eight minipigs were randomized into 2 groups: the Φ 8.5 mm full-thickness chondral defect group (8.5FT group) and the Φ 6.5 mm full-thickness chondral defect group (6.5FT group). The Φ 8.5 mm or Φ 6.5 mm full-thickness chondral defects were prepared in the medial femoral condyle. Knee magnetic resonance imaging (MRI) was performed before sacrifice. India ink staining was performed to macroscopically assess kissing lesions. Histologic staining (hematoxylin-eosin [HE], safranin O/fast green, toluidine blue staining) and immunohistochemistry (collagen I, collagen II, collagen X, MMP-3) were performed. Microcomputed tomography analysis was completed to assess subchondral bone alterations. **Results.** Obvious kissing lesions were observed on the tibial plateau. Knee MRI demonstrated high cartilage signal intensity in the medial femoral condyle and opposite tibial plateau. HE staining demonstrated cartilage fibrillation and prominent cell death. The depletion of safranin O, toluidine blue staining, and collagen II was observed in the kissing lesion areas. The kissing lesion areas demonstrated increased collagen I, Collagen X, and MMP-3 expression. The 8.5FT group showed a significantly lower mean trabecular number (2.80 1/mm) than the control group (3.26 1/mm). The 6.5FT group showed a significantly increased mean trabecular thickness (0.54 mm) and a decreased mean trabecular number (2.71 1/mm) compared to the control group (0.32 mm; 3.26 1/mm). **Conclusions.** The presented findings support the development of kissing lesions caused by full-thickness chondral defects.

Keywords

full-thickness cartilage defect, kissing lesions, subchondral bone remodeling, knee joint

Introduction

Kissing lesions on the opposing cartilage are an important negative effect caused by cartilage defects. Biomechanical alterations have been reported to potentially cause the subsequent development of kissing lesions after cartilage defects. Elevated strain magnitudes were observed in the cartilage opposing the focal full-thickness defect during *in vitro* mechanical tests of bovine osteochondral blocks.¹ Marchi *et al.*² reported that lateral femoral defects increased the maximum compressive strains of tibial cartilage by 25% by using finite element models. Moreover, a bipolar lesion (kissing lesion) is one of the factors related to inferior clinical outcomes in cartilage restoration procedures, such as autologous chondrocyte implantation.^{3,4}

The objective of the present study was to assess the development of a kissing lesion 12 months after the generation of full-thickness chondral defects on the medial femoral condyle in a porcine model. In our study, magnetic resonance imaging (MRI) was performed to assess knee

¹State Key Laboratory of Pharmaceutical Biotechnology, Department of Sports Medicine and Adult Reconstructive Surgery, Nanjing Drum Tower Hospital, The Affiliated Hospital of Nanjing University Medical School, Nanjing, Jiangsu, China

²Laboratory for Bone and Joint Disease, Model Animal Research Center (MARC), Nanjing University, Nanjing, Jiangsu, China

*These authors contributed equally to this work.

Corresponding Authors:

Qing Jiang, State Key Laboratory of Pharmaceutical Biotechnology, Department of Sports Medicine and Adult Reconstructive Surgery, Nanjing Drum Tower Hospital, The Affiliated Hospital of Nanjing University Medical School, 321 Zhongshan Road, Nanjing, Jiangsu 210008, China.
Email: qingj@nju.edu.cn

Dongquan Shi, State Key Laboratory of Pharmaceutical Biotechnology, Department of Sports Medicine and Adult Reconstructive Surgery, Nanjing Drum Tower Hospital, The Affiliated Hospital of Nanjing University Medical School, 321 Zhongshan Road, Nanjing, Jiangsu 210008, China.
Email: shidongquan1215@163.com

joint conditions from images. Histological staining was performed to assess cartilage morphology and glycosaminoglycan (GAG) content. Immunohistochemical staining was performed to assess the expression of collagen I, collagen II, collagen X, and MMP-3. Microcomputed tomography (μ CT) scanning was performed to assess subchondral bone alterations. We hypothesized that kissing lesions developed in the presence of full-thickness chondral defects.

Methods

Study Design and Surgical Procedure

All experiments were approved by the Institutional Laboratory Animal Ethics Committee of Nanjing Drum Tower Hospital, Nanjing, and carried out in accordance with the National Institutes of Health Guide for the Care and Use of Laboratory Animals. Eight mature minipigs (Bama minipig, female, 40 ± 10 kg) were randomized into 2 groups: the $\Phi 6.5$ mm full-thickness chondral defect group (6.5FT group, $n = 4$) and the $\Phi 8.5$ mm full-thickness chondral defect group (8.5FT group, $n = 4$). The left knees of the 8.5FT group served as the control group ($n = 4$).

Induced anesthesia was performed by intramuscular injection of atropine (0.02 mL/kg), xylazine hydrochloride (0.2 mL/kg), and droperidol (0.2 mg/kg). Anesthesia was maintained with the use of an intravenous infusion of propofol. Then, the minipigs were placed in the supine position after general anesthesia. Normal ventilation was maintained by endotracheal intubation and mechanical ventilation with a tidal volume of 300 mL. The medial parapatellar approach was used to achieve external dislocation of the patella. Then, the medial femoral condyle (**Fig. 1A1**) was exposed under sterile conditions. Full-thickness chondral defects with the subchondral bone plate intact measuring $\Phi 6.5$ mm or $\Phi 8.5$ mm were prepared in the medial femoral condyle weight-bearing area of right knees by using osteochondral transplantation instrumentation (**Fig. 1B1** and **C1**). The minipigs were permitted to move freely in a comfortable environment for 1 year.

Macroscopic Evaluation and Outerbridge Grading

At the 12-month follow-up, all minipigs were sacrificed by intravenous injection of propofol, and the knee joints were harvested. The macroscopic view of the femoral condyles, meniscus, and tibial plateau was assessed after removal of the soft tissue. Gross changes in the medial tibial plateau articular surface were rated according to the Outerbridge classification (**Table 1**).⁵ India ink staining was used to highlight the kissing lesions on the opposite tibial plateau including cartilage erosion, fibrillation, and cracks according to the criteria of Meachim.⁶

MRI Acquisition

At the 12-month follow-up after the operation, knee MRI was completed using a 3.0 T MRI Scanner (United Imaging, China) to obtain high-resolution MRI images before sacrifice. The images in the sagittal plane covering the medial knee compartment were selected to evaluate the joint condition.

μ CT Analysis

For evaluation of subchondral bone alterations below the full-thickness chondral defect on the medial femoral condyle and kissing lesions on the opposite tibial plateau, μ CT scanning was performed. The medial femoral condyle and medial tibial plateau were cut into blocks covering the original defect area or kissing lesion area. Then, the specimens were wrapped with parafilm and scanned with a μ CT scanner (Scanco Medical AG, Switzerland). For assessment of the subchondral bone alterations below the full-thickness chondral defect, a rectangular region of interest (ROI) measuring 1 mm in depth below the original defect area was drawn to determine the analyzed region (**Fig. 3a**). For assessment of subchondral bone alterations below kissing lesions on the opposite tibial plateau, a rectangular region of interest (ROI) measuring 1 mm in depth below the kissing lesion area (the macroscopic view demonstrated kissing lesions were mainly distributed in the lateral 1/2 portion of the medial tibial plateau) was drawn to determine the analyzed region (**Fig. 3b**). Then, quantitative analysis of the percentage of bone volume (BV/TV, %), bone mineral density (BMD, g/cm³), trabecular thickness (Tb.Th, mm), trabecular number (Tb.N, 1/mm), and trabecular separation (Tb.Sp, mm) was performed.⁷

Histology and OARSI Scoring

After μ CT scanning, the osteochondral blocks of the tibial plateau covering the kissing lesion area were fixed with 10% formalin for at least 24 hours. The decalcification was completed with 15% ethylenediaminetetraacetic acid for 60 days. The samples were embedded in paraffin and then cut into sections of 3 μ m. The cartilage morphology was assessed by HE staining. The glycosaminoglycan (GAG) content was assessed by toluidine blue staining and safranin O/fast green staining. Then, the stained sections were observed with a light microscope (Zeiss, Germany). The osteoarthritis cartilage histopathology assessment system (OARSI system; **Table 2**) described by Pritzker *et al.*⁸ was used to perform the histological analysis. Six grades were included in the OARSI system. Grade 0 indicates an intact surface and cartilage morphology; Grade 1 indicates an uneven but intact surface; Grade 2 indicates surface discontinuity; Grade 3 indicates vertical

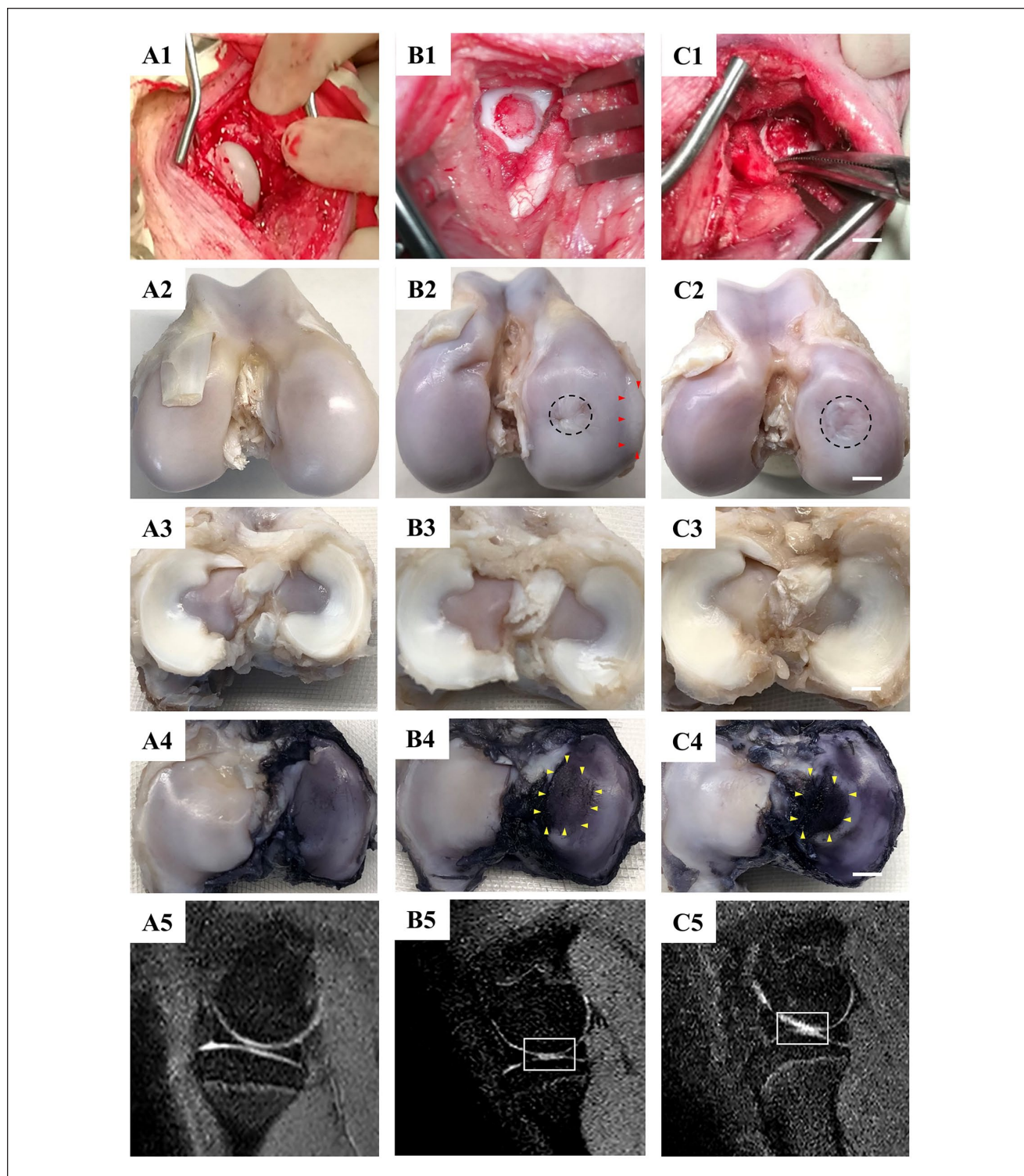


Figure 1. The outcomes of macroscopic and MRI evaluation. **(A1-A5)** samples of the control group; **(B1-B5)** samples of the 6.5FT group; **(C1-C5)** samples of the 8.5FT group; **(A1, B1, C1)** macroscopic view of the medial femoral condyle during the operation, scale bar: 5 mm. **(A2, B2, C2)** macroscopic view of the medial femoral condyle at 12 months postoperatively. The area surrounded by red triangles represents osteophytes. The black dotted circle represents the original defect margin. **(A3, B3, C3)** macroscopic view of the meniscus at 12 months postoperatively. **(A4, B4, C4)** macroscopic view of the opposite tibial plateau articular surface with India ink staining at 12 months postoperatively. The area surrounded by yellow triangles represents the kissing lesions. **(A5, B5, C5)** MRI images of the knee medial femoral condyle. The white rectangle represents the region of interest of cartilage edema with a high signal intensity.

Table 1. Outerbridge Classification.

Grade	Pathology
I	Softening and swelling of articular cartilage
II	Fragmentation and fissuring of articular cartilage affecting an area of less than 0.5 inches
III	Fragmentation and fissuring of articular cartilage affecting an area greater than 0.5 inches
IV	Cartilage erosion to bone

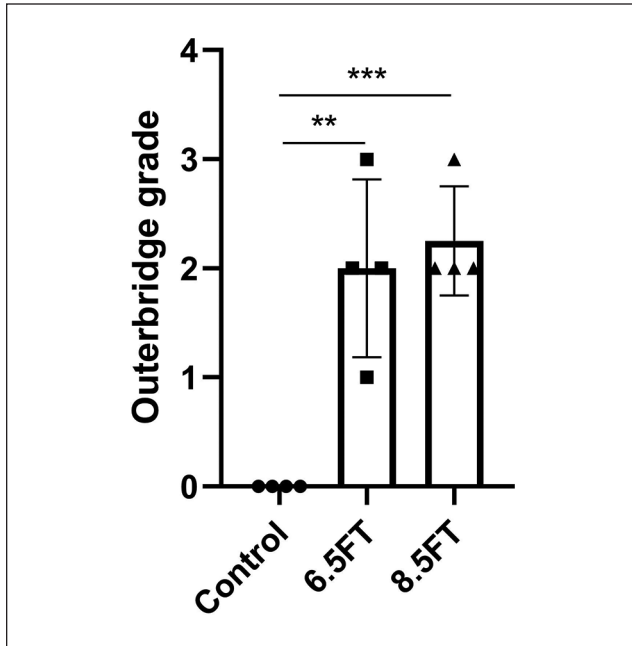


Figure 2. The outcomes of Outerbridge grade. 6.5FT: Φ 6.5 mm full-thickness chondral defect group, 8.5FT: Φ 8.5 mm full-thickness chondral defect group. The results are presented as the mean \pm standard deviation. **, $P < 0.01$; ***, $P < 0.0005$.

fissures; Grade 4 indicates cartilage erosion; Grade 5 indicates denudation; and Grade 6 indicates deformation.

Immunohistochemistry

For immunohistochemistry, primary antibodies, for example, rabbit anti-Collagen I (Abcam, ab34710, Cambridge, UK), rabbit anti-Collagen II (Abcam, ab34712, Cambridge, UK), mouse anti-Collagen X (Abcam, ab49945, Cambridge, UK), and rabbit anti-MMP-3 (Bioss, bs-0413R, Woburn, MA) antibodies were used. Secondary antibodies included goat anti-rabbit IgG H&L (HRP; Abcam, ab6721, Cambridge, UK) and goat anti-mouse IgG H&L (HRP; Abcam, ab6789, Cambridge, UK). The sections containing superficial cartilage and subchondral bone were incubated with 0.4% pepsin (Aladdin, P110928, Shanghai, China) at

37°C for 1 hour for antigen retrieval. Endogenous peroxidase was blocked by 3% H_2O_2 , and nonspecific protein binding was blocked by goat serum (Boster, AR0009, China). Primary antibodies were used overnight incubation at 4°C followed by incubation with secondary antibodies for 1 hour at room temperature. Finally, a DAB kit was used to develop the color.

Statistical Analysis

The data are summarized by descriptive statistics. All data are presented as the mean and standard deviation (SD). Statistical analysis was completed by GraphPad Prism 8.0.1 (GraphPad Software, Inc., La Jolla, CA). The statistical analysis was performed with an unpaired *t* test or Mann-Whitney test according to the results of the normality tests. $P < 0.05$ was considered statistically significant.

Results

Macroscopic, MRI Evaluation, and Outerbridge Grading

At 12 months postoperatively, the full-thickness chondral defects of the 8.5FT and 6.5FT groups showed varying degrees of repair. However, compared to the normal control group (Fig. 1A2), obvious uneven cartilage surface, fibrillation, and demarcating borders were observed in the repaired tissue of the 6.5FT group (Fig. 1B2) and the 8.5FT group (Fig. 1C2). Medial femoral condyle flattening or deformation was observed in the 6.5FT and 8.5FT groups. Moreover, osteophyte formation was observed in one sample of the 6.5FT group (Fig. 1B2). Similar to the normal meniscus (Fig. 1A3), no obvious medial meniscus injuries were observed in the 6.5FT group (Fig. 1B3) or the 8.5FT group (Fig. 1C3) at 12 months postoperatively. India ink staining was used to highlight kissing lesions on the opposite tibial plateau. Higher levels of India ink indicate more severe cartilage abrasions. As demonstrated by Figure 1B4 and C4, more India ink remained in the chondral defect group than in the control group (Fig. 1A4). The kissing lesions on the tibial plateau exhibited cartilage abrasions, fragmentation, and fissuring. As shown by MRI images, the 6.5FT (Fig. 1B5) and 8.5FT (Fig. 1C5) groups demonstrated higher cartilage signal intensity in the medial femoral condyle and the opposite tibial plateau than the control group (Fig. 1A5), indicating abnormal cartilage edema. Moreover, the 6.5FT and 8.5FT groups demonstrated significantly higher Outerbridge grades than the control group (Fig. 2).

μ CT Scanning and Subchondral Bone Evaluation

Compared to that of the peripheral native subchondral bone plate, the thickness of the subchondral bone plate below the

Table 2. Osteoarthritis Cartilage Histopathology Grade Assessment.

Grade (Key Feature)	Associated Criteria (Tissue Reaction)
Grade 0: surface intact, cartilage morphology intact	Matrix: normal architecture
Grade 1: surface intact	Cells: intact, appropriate orientation Matrix: superficial zone intact, edema, and/or fibrillation (abrasion), focal superficial matrix condensation Cells: death, proliferation (clusters), hypertrophy, superficial zone reaction must be more than superficial fibrillation only
Grade 2: surface discontinuity	As above + Matrix discontinuity at superficial zone (deep fibrillation) ± Cationic stain matrix depletion (safranin O or toluidine blue) upper 1/3 of cartilage ± Focal perichondronal increased stain (mid zone) ± Disorientation of chondron columns
Grade 3: vertical fissures	Cells: death, proliferation (clusters), hypertrophy As above Matrix vertical fissures into mid zone, branched fissures ± Cationic stain depletion (safranin O or toluidine blue) into lower 2/3 of cartilage (deep zone) ± New collagen formation (polarized light microscopy, picro sirius red stain) Cells: death, regeneration (clusters), hypertrophy, cartilage domains adjacent to fissures
Grade 4: erosion	Cartilage matrix loss: delamination of superficial layer, mid layer cyst formation Excavation: matrix loss superficial layer and mid zone
Grade 5: denudation	Surface: sclerotic bone or reparative tissue including fibrocartilage within denuded surface; microfracture with repair limited to bone surface
Grade 6: deformation	Bone remodeling (more than osteophyte formation only); includes microfracture with fibrocartilaginous and osseous repair extending above the previous surface

full-thickness chondral defect increased at 12 months post-operatively (**Fig. 3a**). The 6.5FT group showed a significantly increased mean trabecular thickness (0.54 mm) and a decreased mean trabecular number (2.71 1/mm) compared to the control group (0.32 mm; 3.26 1/mm) in the ROI below the full-thickness chondral defect. The 8.5FT group showed a significantly lower mean trabecular number (2.80 1/mm) than the control group (3.26 1/mm) in the ROI below the full-thickness chondral defect (**Fig. 3c**). The control group and experimental groups showed no significant differences in BMD, BV/TV, Tb.Th, Tb.N, and Tb.Sp in the ROI of the opposite tibial plateau (**Fig. 3d**).

Histology, Immunohistochemistry Evaluation, and OARSI Grading

Tissue abnormalities were assessed by histology and immunohistochemistry. HE staining of native articular cartilage demonstrated an intact and smooth surface and a well-organized matrix and chondrocytes (**Fig. 4A1**). In the 6.5FT (**Fig. 4B1**) and 8.5FT (**Fig. 4C1**) groups, cartilage superficial fibrillation and vertical fissures or erosion occurred, and prominent cell death and hypertrophy were also observed. As shown in **Figure 4A2** and **A3**, homogeneous safranin O or toluidine blue staining was demonstrated in the native control group. The depletion of safranin O or toluidine blue

staining in the kissing lesion area was observed in the 6.5FT (**Fig. 4B2** and **B3**) and 8.5FT (**Fig. 4C2** and **C3**) groups, indicating reduced GAG content. Compared with the control group (**Fig. 4A4**), the 6.5FT (**Fig. 4B4**) and 8.5FT (**Fig. 4C4**) groups demonstrated reduced collagen II expression in the cartilage layer. Moreover, the 6.5FT and 8.5FT groups demonstrated higher collagen I (**Fig. 4B5** and **C5**), collagen X (**Fig. 4B6** and **C6**), and MMP-3 (**Fig. 4B7** and **C7**) expression than the control group (**Fig. 4A5-A7**). For OARSI grading of cartilage degeneration, Grade 0 indicated normal cartilage (**Fig. 5A**), and Grades 1 to 4 were observed in the present study (**Fig. 5B-E**). The OARSI grade of the 6.5FT and 8.5FT groups significantly exceeded that of the control group (**Fig. 5F**).

Discussion

Previous studies have mainly concentrated on the perilesional cartilage changes caused by focal osteochondral defects.⁹⁻¹¹ The present study verified the occurrence of kissing lesions on the opposite tibial plateau and subchondral bone alterations below full-thickness chondral defects at the 12-month follow-up. The kissing lesions showed cartilage abrasions, fragmentation, and fissuring with increased India ink staining and an abnormal signal intensity on MRI of the cartilage. The reduced GAG content and collagen II

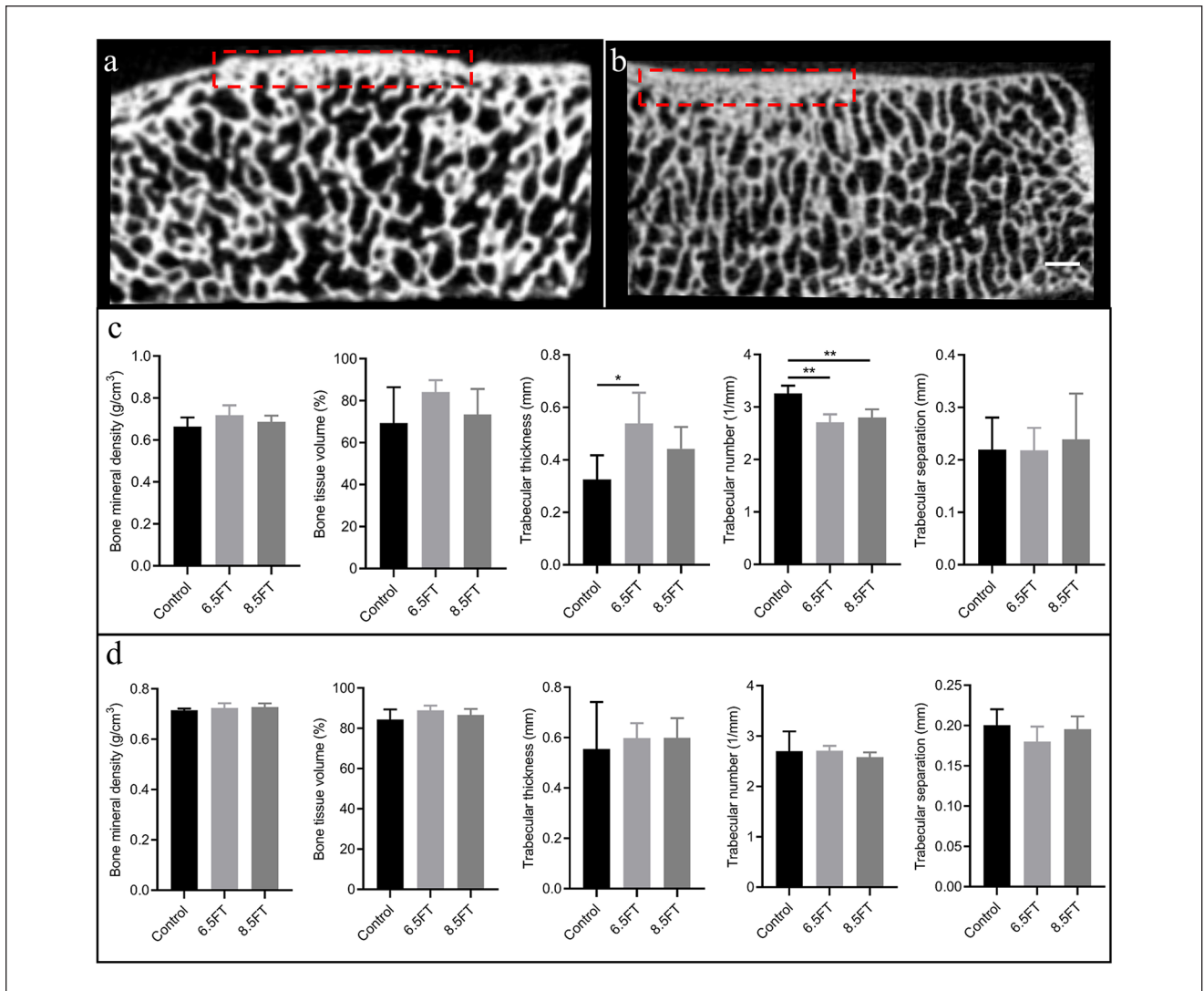


Figure 3. Schematic of subchondral bone analysis and outcomes of quantitative analysis. (a) Analysis of subchondral bone alterations 1 mm below the full thickness chondral defect. The red dotted rectangular region of interest (ROI) measuring 1 mm in depth below the original chondral defect area represents the analyzed region. (b) Analysis of subchondral bone alterations below kissing lesions on the opposite tibial plateau. The red dotted rectangular region of interest (ROI) measuring 1 mm in depth below the kissing lesion area (the gross view demonstrated that the kissing lesions were mainly distributed in the lateral 1/2 portion of the medial tibial plateau) represents the analyzed region. Scale bar: 1 mm. (c) Quantitative analysis of the aforementioned subchondral bone below the original chondral defect area. (d) Quantitative analysis of the aforementioned subchondral bone below kissing lesions on the opposite tibial plateau. The results are presented as the mean \pm standard deviation. *, $P < 0.05$; **, $P < 0.01$.

content demonstrated by cartilage-specific staining reflected the degradation of the cartilage matrix. The increased collagen I, collagen X, and MMP-3 expression demonstrated by immunohistochemistry indicated cartilage fibrillation, hypertrophy, and inflammatory catabolic cytokine generation, respectively.¹² Cartilage homeostasis was disrupted in the kissing lesions.

Mechanical effects have been suggested to be a mechanism that initiates subsequent cartilage degeneration caused by cartilage defects. The flattening and

deformation of the medial femoral condyle was observed in the present study, which was consistent with previous studies.^{10,13} Jackson *et al.*¹⁰ performed a preliminary study on the intrinsic healing of full-thickness cartilage defects in a goat model. The research also found cartilage flattening and deformation surrounding the defect. Braman *et al.*¹³ found that abnormal flattening and deformation were histologically observed in the cartilage adjacent to and opposite to the medial femoral condyle cartilage defects of loaded rabbit knee joints. This abnormal

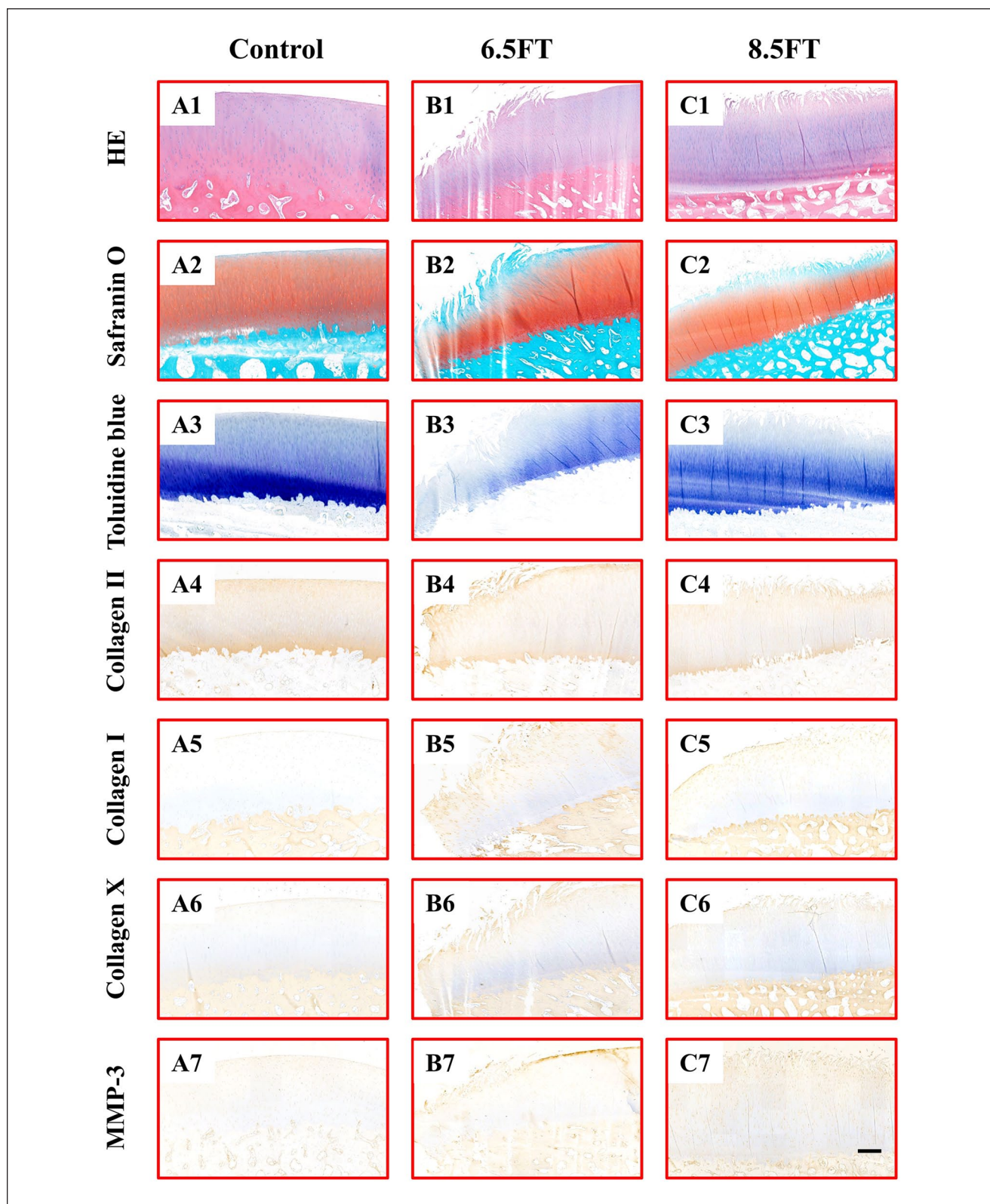


Figure 4. Histology and immunohistochemistry staining. Control: native control group (**A1-A7**); 6.5FT: Φ 6.5 mm full-thickness chondral defect group (**B1-B7**); 8.5FT: Φ 8.5 mm full-thickness chondral defect group (**C1-C7**). Scale bar: 500 μ m.

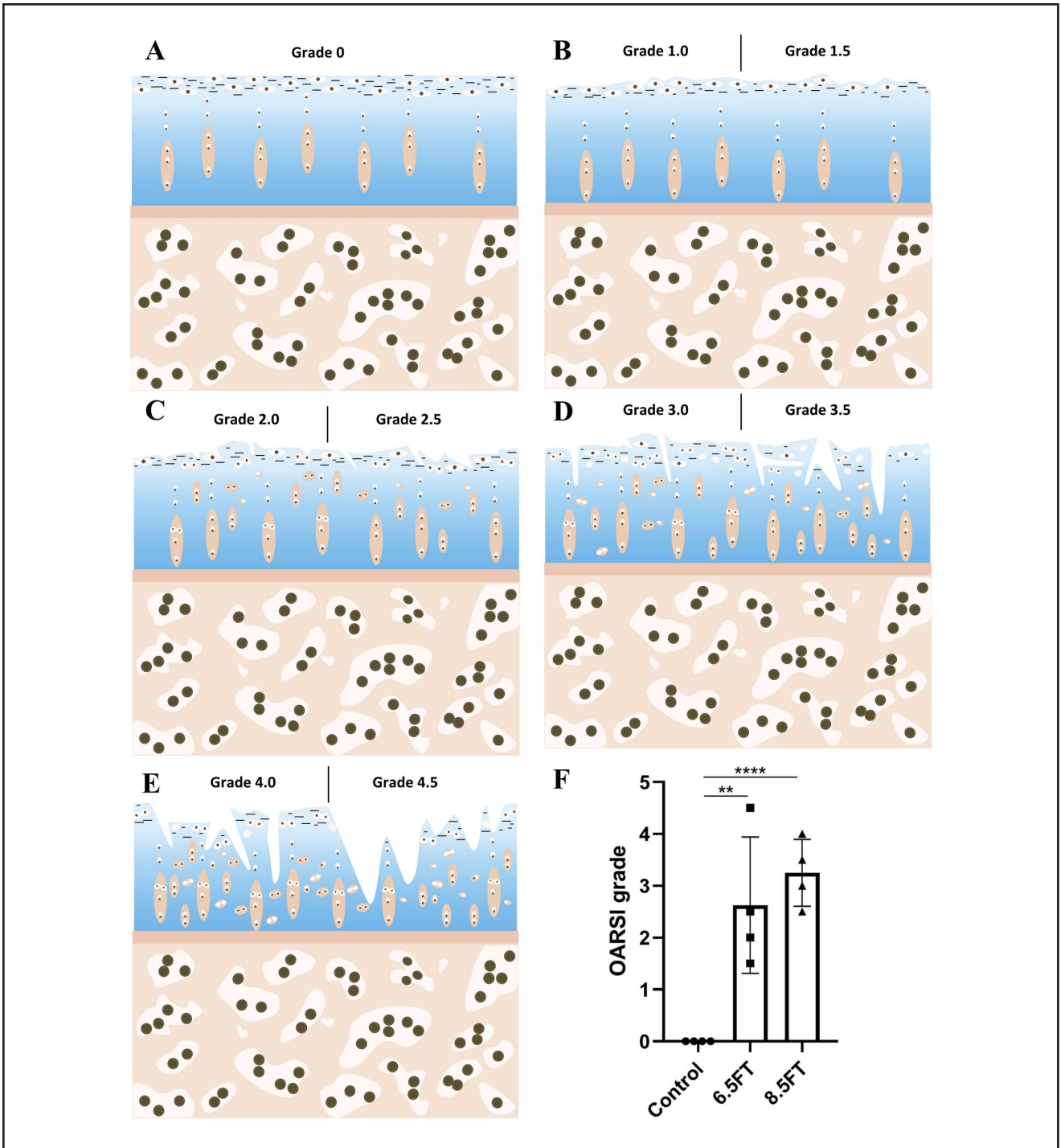


Figure 5. Schematics and outcomes of OARSI grading. **(A-E):** Schematics of OARSI Grades 0 to 4. Grade 0: the surface is intact and smooth. Matrix and chondrocytes are well organized. Grade 1: intact but uneven surface demonstrated by fibrillation. Cell death or proliferation may be accompanied. Grade 1.0: cell intact; Grade 1.5: cell death. Grade 2: surface interrupted. Fibrillation extends deeper. Cell death, proliferation and hypertrophy may be accompanied. Grade 2.0: fibrillation through the superficial zone; Grade 2.5: surface abrasion with matrix loss within the superficial zone. Grade 3: vertical fissures extend to the middle zone. Fibrillation extends to the middle zone. Cell death and proliferation may be accompanied mainly adjacent to fissures. Grade 3.0: simple fissures; Grade 3.5: branched or complex fissures. Grade 4: cartilage erosion. Cartilage matrix loss and cyst formation within the cartilage matrix. Grade 4.0: superficial zone delamination; Grade 4.5: mid-zone excavation.⁸ **(F):** The outcomes of OARSI grading. The results are presented as the mean \pm standard deviation. **, $P < 0.01$; ****, $P < 0.0001$.



Figure 6. The exhibition of kissing lesions in the clinic was demonstrated by MRI images of a patient with early OA (female, 55 years old). The white ellipse represents concomitant cartilage lesions in the medial femoral condyle and the opposite tibial plateau. MFC = medial femoral condyle; MTP = medial tibial plateau.

condylar flattening and deformation may be attributed to the recruitment of adjacent cartilage to counteract the reduced cartilage contact area caused by focal defects, thus resulting in condylar flattening and deformation.¹⁴ Moreover, the subsequent mismatch between femoral and tibial condyles caused by abnormal tissue deformation would weaken the load support of interstitial fluid, which could lead to increased load on the solid matrix.¹⁵ Dabiri and Li¹⁶ also concluded that focal chondral defects compromised fluid-pressure dependent load support in the knee. Many previous studies have shown that abnormal excessive mechanical load leads to cartilage matrix degradation¹⁷⁻¹⁹ and chondrocyte apoptosis.^{20,21} Furthermore, Gratz *et al.*¹ found elevated strain magnitudes in the cartilage surrounding and opposing the focal full-thickness defect during *in vitro* mechanical tests of bovine osteochondral blocks. The excess strain magnitude and rate may contribute to the initiation of cartilage damage.^{17,22} The altered mechanical signals generated from abnormal mechanical loading could affect joint homeostasis at the cellular level.²³ Hunziker and Quinn²⁴ found irreversible loss of chondrocyte volume and compromised anabolic activity of chondrocytes surrounding partial-thickness focal cartilage defects in rabbit and miniature pig models. In addition, residual viable chondrocytes may demonstrate abnormal metabolic activity after injurious mechanical effects.^{17,25} Moreover, the uneven surface at the defect site

inherently resulted in cartilage abrasions on the opposite tibial plateau during the rolling motion of the knee joint.

Subchondral bone alterations accompany the progression of OA.^{7,26-28} Chen *et al.*²⁹ found significantly reduced subchondral trabecular number and increased trabecular thickness in knee samples from patients with progressive OA. The research further observed trabecular number loss and trabecular thickening in an established guinea pig model of spontaneous OA. Interestingly, the subchondral bone alterations below the full-thickness chondral defect observed in our study were consistent with their findings. However, in our study, no significant differences were observed between the control group and experimental group in terms of subchondral bone parameters on the opposite tibial plateau. The discrepancies to their findings may be attributed to the limited sample size or observation period. Combined with subchondral bone alterations and kissing lesions on the opposite tibial plateau, for example, cartilage abrasions, fissures, and increased collagen I, collagen X, and MMP-3 expression, definite OA development occurred due to focal cartilage defects at 1 year postoperatively. Moreover, Schinhan *et al.*³⁰ summarized the unicompartamental development of knee OA caused by focal critical sized cartilage defects in an ovine model at 12 weeks postoperatively. The subchondral bone alterations after surgically prepared cartilage defects may be attributed to osteochondral unit damage. The osteochondral unit, which is composed of articular cartilage, calcified cartilage, and subchondral bone, appears to possess a unique capacity to transfer loads in the knee joint.³¹ The subchondral bone provides support to the superficial cartilage in distributing joint loads. However, subchondral bone lesions could alter their load distribution capacities, resulting in subsequent cartilage lesions through abnormal mechanical loading.³² Conversely, prior cartilage lesions contribute to subsequent subchondral bone alterations and remodeling.³³ However, the specific mechanisms remain to be elucidated.

Bipolar cartilage lesions are a common morbidity in the clinic, especially for patients with OA. In **Figure 6**, the clinically concomitant medial femoral condylar cartilage lesion and opposite tibial plateau cartilage lesion was observed in a patient with early OA (female, 55 years old). The presented findings in our study support the development of kissing lesions and subchondral bone alterations in the presence of full-thickness cartilage lesions. Timely management should be performed to prevent or delay the development of kissing lesions, if a unipolar cartilage lesion is diagnosed in the clinic. Full-thickness cartilage lesions have been verified to be important independent predictive factors for progression to total knee arthroplasty in older adults with minimal to moderate OA.³⁴ Moreover, a bipolar lesion (kissing lesion) is regarded as one of the factors related to inferior clinical outcomes in cartilage restoration

procedures, such as autologous chondrocyte implantation³ and osteochondral allograft transplantation.³⁵

Some limitations exist in the present study. First, the sample size was limited in the present study. Because a large animal model has a high space and cost requirement, the sample size for each group in the present study was four. Second, although the present study demonstrated alterations in trabecular thickness and number in the subchondral bone below the chondral defects, micro-architectural alterations in the subchondral bone, such as rod-like and plate-like trabecular alterations, were not demonstrated. Third, the present study only demonstrated kissing lesions and subchondral bone remodeling in the weight-bearing area of the medial compartment. However, kissing lesions or subchondral bone remodeling in the non-weight-bearing area, such as the patellofemoral joint, was not demonstrated. Finally, the mechanisms of subchondral bone remodeling after focal cartilage defects have not been elucidated.

Conclusions

In summary, the presented findings support the development of a kissing lesion caused by a full-thickness chondral defect.

Authors' Note

This work was done in Nanjing Drum Tower Hospital, Nanjing, China.

Author Contributions

WY and XX contributed to conceptualization, methodology, validation, formal analysis, investigation, data curation, original draft, and revision. QX, ZS, and ZL contributed to methodology, validation, data curation, original draft, and revision. RW and WY contributed to data curation, original draft, and revision. QJ and DS contributed to conceptualization, original draft and revision, review and editing, and supervision.

Acknowledgments and Funding

The author(s) disclosed receipt of the following financial support for the research, authorship, and/or publication of this article: This work was supported by National Key R&D Program of China (2018YFC1105904), Key Program of NSFC (81730067), Excellent Young Scholars NSFC (81622033), National Science Foundation of China (81802196), Natural Science Foundation of Jiangsu Province, China (BK20180127), Jiangsu Provincial Key Medical Center Foundation, Jiangsu Provincial Medical Outstanding Talent Foundation, Jiangsu Provincial Medical Youth Talent Foundation, and Jiangsu Provincial Key Medical Talent Foundation.

Declaration of Conflicting Interests

The author(s) declared no potential conflicts of interest with respect to the research, authorship, and/or publication of this article.

Ethical Approval

All experiments were approved by the Institutional Laboratory Animal Ethics Committee of Nanjing Drum Tower Hospital, Nanjing, and carried out in accordance with the National Institutes of Health Guide for the Care and Use of Laboratory Animals.

Animal Welfare

The present study followed international, national, and/or institutional guidelines for humane animal treatment and complied with relevant legislation.

ORCID iD

Dongquan Shi  <https://orcid.org/0000-0002-4769-7816>

References

1. Gratz KR, Wong BL, Bae WC, Sah RL. The effects of focal articular defects on cartilage contact mechanics. *J Orthop Res*. 2009;27(5):584-92. doi:10.1002/jor.20762
2. Marchi BC, Arruda EM, Coleman R. The effect of articular cartilage focal defect size and location in whole knee biomechanics models. *J Biomech Eng*. Epub Jun 15, 2019. doi:10.1115/1.4044032
3. Peterson L, Vasiliadis HS, Brittberg M, Lindahl A. Autologous chondrocyte implantation: a long-term follow-up. *Am J Sports Med*. 2010;38(6):1117-24. doi:10.1177/0363546509357915
4. Seo SS, Kim CW, Jung DW. Management of focal chondral lesion in the knee joint. *Knee Surg Relat Res*. 2011;23(4):185-96. doi:10.5792/ksrr.2011.23.4.185
5. Outerbridge RE. The etiology of chondromalacia patellae. *J Bone Joint Surg Br*. 1961;43-B:752-7.
6. Meachim G. Light microscopy of Indian ink preparations of fibrillated cartilage. *Ann Rheum Dis*. 1972;31(6):457-64. doi:10.1136/ard.31.6.457
7. Wang T, Wen CY, Yan CH, Lu WW, Chiu KY. Spatial and temporal changes of subchondral bone proceed to microscopic articular cartilage degeneration in guinea pigs with spontaneous osteoarthritis. *Osteoarthritis Cartilage*. 2013;21(4):574-81. doi:10.1016/j.joca.2013.01.002
8. Pritzker KP, Gay S, Jimenez SA, Ostergaard K, Pelletier JP, Revell PA, *et al*. Osteoarthritis cartilage histopathology: grading and staging. *Osteoarthritis Cartilage*. 2006;14(1):13-29. doi:10.1016/j.joca.2005.07.014
9. Hepp P, Osterhoff G, Niederhagen M, Marquass B, Aigner T, Bader A, *et al*. Perilesional changes of focal osteochondral defects in an ovine model and their relevance to human osteochondral injuries. *J Bone Joint Surg Br*. 2009;91(8):1110-9. doi:10.1302/0301-620X.91B8.22057
10. Jackson DW, Lalor PA, Aberman HM, Simon TM. Spontaneous repair of full-thickness defects of articular cartilage in a goat model. A preliminary study. *J Bone Joint Surg Am*. 2001;83(1):53-64. doi:10.2106/00004623-200101000-00008
11. Bail H, Klein P, Kolbeck S, Krummrey G, Weiler A, Schmidmaier G, *et al*. Systemic application of growth hormone enhances the early healing phase of osteochondral defects—a preliminary study in micropigs. *Bone*. 2003;32(5):457-67. doi:10.1016/s8756-3282(03)00051-6

12. Fernandes JC, Martel-Pelletier J, Pelletier JP. The role of cytokines in osteoarthritis pathophysiology. *Biorheology*. 2002;39(1-2):237-46.
13. Braman JP, Bruckner JD, Clark JM, Norman AG, Chansky HA. Articular cartilage adjacent to experimental defects is subject to atypical strains. *Clin Orthop Relat Res*. 2005(430):202-7. doi:10.1097/01.blo.0000145990.58146.3d
14. Brown TD, Pope DF, Hale JE, Buckwalter JA, Brand RA. Effects of osteochondral defect size on cartilage contact stress. *J Orthop Res*. 1991;9(4):559-67. doi:10.1002/jor.1100090412
15. Ateshian GA, Wang H. A theoretical solution for the frictionless rolling contact of cylindrical biphasic articular cartilage layers. *J Biomech*. 1995;28(11):1341-55. doi:10.1016/0021-9290(95)00008-6
16. Dabiri Y, Li L. Focal cartilage defect compromises fluid-pressure dependent load support in the knee joint. *Int J Numer Method Biomed Eng*. 2015;31(6). doi:10.1002/cnm.2713
17. Quinn TM, Allen RG, Schalet BJ, Perumbuli P, Hunziker EB. Matrix and cell injury due to sub-impact loading of adult bovine articular cartilage explants: effects of strain rate and peak stress. *J Orthop Res*. 2001;19(2):242-9. doi:10.1016/S0736-0266(00)00025-5
18. Wilson W, van Burken C, van Donkelaar C, Buma P, van Rietbergen B, Huiskes R. Causes of mechanically induced collagen damage in articular cartilage. *J Orthop Res*. 2006;24(2):220-8. doi:10.1002/jor.20027
19. Thibault M, Poole AR, Buschmann MD. Cyclic compression of cartilage/bone explants in vitro leads to physical weakening, mechanical breakdown of collagen and release of matrix fragments. *J Orthop Res*. 2002;20(6):1265-73. doi:10.1016/S0736-0266(02)00070-0
20. D'Lima DD, Hashimoto S, Chen PC, Lotz MK, Colwell CW. Cartilage injury induces chondrocyte apoptosis. *J Bone Joint Surg Am*. 2001;83-A Suppl 2(Pt 1):19-21. doi:10.2106/00004623-200100021-00004
21. Patwari P, Gaschen V, James IE, Berger E, Blake SM, Lark MW, *et al*. Ultrastructural quantification of cell death after injurious compression of bovine calf articular cartilage. *Osteoarthritis Cartilage*. 2004;12(3):245-52. doi:10.1016/j.joca.2003.11.004
22. Bae WC, Schumacher BL, Sah RL. Indentation probing of human articular cartilage: effect on chondrocyte viability. *Osteoarthritis Cartilage*. 2007;15(1):9-18. doi:10.1016/j.joca.2006.06.007
23. Andriacchi TP, Favre J. The nature of in vivo mechanical signals that influence cartilage health and progression to knee osteoarthritis. *Curr Rheumatol Rep*. 2014;16(11):463. doi:10.1007/s11926-014-0463-2
24. Hunziker EB, Quinn TM. Surgical removal of articular cartilage leads to loss of chondrocytes from cartilage bordering the wound edge. *J Bone Joint Surg Am*. 2003;85-A(Suppl 2):85-92. doi:10.2106/00004623-200300002-00011
25. Kurz B, Jin M, Patwari P, Cheng DM, Lark MW, Grodzinsky AJ. Biosynthetic response and mechanical properties of articular cartilage after injurious compression. *J Orthop Res*. 2001;19(6):1140-6. doi:10.1016/s0736-0266(01)00033-x
26. Kuroki K, Cook CR, Cook JL. Subchondral bone changes in three different canine models of osteoarthritis. *Osteoarthritis Cartilage*. 2011;19(9):1142-9. doi:10.1016/j.joca.2011.06.007
27. Intema F, Sniekers YH, Weinans H, Vianen ME, Yocum SA, Zuurmond AM, *et al*. Similarities and discrepancies in subchondral bone structure in two differently induced canine models of osteoarthritis. *J Bone Miner Res*. 2010;25(7):1650-7. doi:10.1002/jbmr.39
28. Intema F, Hazewinkel HA, Gouwens D, Bijlsma JW, Weinans H, Lafeber FP, *et al*. In early OA, thinning of the subchondral plate is directly related to cartilage damage: results from a canine ACLT-menisectomy model. *Osteoarthritis Cartilage*. 2010;18(5):691-8. doi:10.1016/j.joca.2010.01.004
29. Chen Y, Hu Y, Yu YE, Zhang X, Watts T, Zhou B, *et al*. Subchondral trabecular rod loss and plate thickening in the development of osteoarthritis. *J Bone Miner Res*. 2018;33(2):316-27. doi:10.1002/jbmr.3313
30. Schinhan M, Gruber M, Vavken P, Dorotka R, Samouh L, Chiari C, *et al*. Critical-size defect induces unicompartmental osteoarthritis in a stable ovine knee. *J Orthop Res*. 2012;30(2):214-20. doi:10.1002/jor.21521
31. Goldring SR, Goldring MB. Changes in the osteochondral unit during osteoarthritis: structure, function and cartilage-bone crosstalk. *Nat Rev Rheumatol*. 2016;12(11):632-44. doi:10.1038/nrrheum.2016.148
32. Ma JX, He WW, Zhao J, Kuang MJ, Bai HH, Sun L, *et al*. Bone microarchitecture and biomechanics of the necrotic femoral head. *Sci Rep*. 2017;7(1):13345. doi:10.1038/s41598-017-13643-2
33. Radin EL, Martin RB, Burr DB, Caterson B, Boyd RD, Goodwin C. Effects of mechanical loading on the tissues of the rabbit knee. *J Orthop Res*. 1984;2(3):221-34. doi:10.1002/jor.1100020303
34. Everhart JS, Abouljoud MM, Kirven JC, Flanigan DC. Full-thickness cartilage defects are important independent predictive factors for progression to total knee arthroplasty in older adults with minimal to moderate osteoarthritis: data from the Osteoarthritis Initiative. *J Bone Joint Surg Am*. 2019;101(1):56-63. doi:10.2106/JBJS.17.01657
35. Familiari F, Cinque ME, Chahla J, Godin JA, Olesen ML, Moatshe G, *et al*. Clinical outcomes and failure rates of osteochondral allograft transplantation in the knee: a systematic review. *Am J Sports Med*. 2018;46(14):3541-9. doi:10.1177/0363546517732531